Electronic Supplementary Information

Remote functionalization in surface-assisted dehalogenation by conformational mechanics: organometallic self-assembly of 3,3',5,5'-tetrabromo-2,2',4,4',6,6'-hexafluorobiphenyl on Ag(111)

Matthias Lischka,[a,b] Georg S. Michelitsch,[c] Natalia Martsinovich,[d] Johanna Eichhorn,[a,b] Atena Rastgoo-Lahrood,[a,b] Thomas Strunskus,[e] Rochus Breuer,[f] Karsten Reuter,[c] Michael Schmittel,[f] and Markus Lackinger [a,b,g]

[a.] *Department of Physics, Technische Universität München, James-Frank-Str. 1, 85748 Garching, Germany. E-mail: markus@lackinger.org*

[b.] *Center for NanoScience (CENS) & Nanosystems-Initiative-Munich, Schellingstr. 4, 80799 München, Germany*

[c.] *Chair for Theoretical Chemistry and Catalysis Research Center, Technische Universität München, Lichtenbergstraße 4, 85747 Garching, Germany*

[d.] *Department of Chemistry, University of Sheffield, Sheffield S3 7HF, U.K.*

[e.] *Institute of Materials Science – Multicomponent Materials, Christian-Albrecht-Universität zu Kiel, Kaiserstr. 2, 24143 Kiel, Germany*

[f.] *Center of Micro- and Nanochemistry and Engineering, Organische Chemie I, Universität Siegen, Adolf-Reichwein-Str. 2, 57068 Siegen, Germany*

[g.] *Deutsches Museum, Museumsinsel 1, 80538 Munich, Germany*

1. Additional STM and XPS data: Br_4F_6BP on Ag(111)

Overview STM images after room-temperature deposition

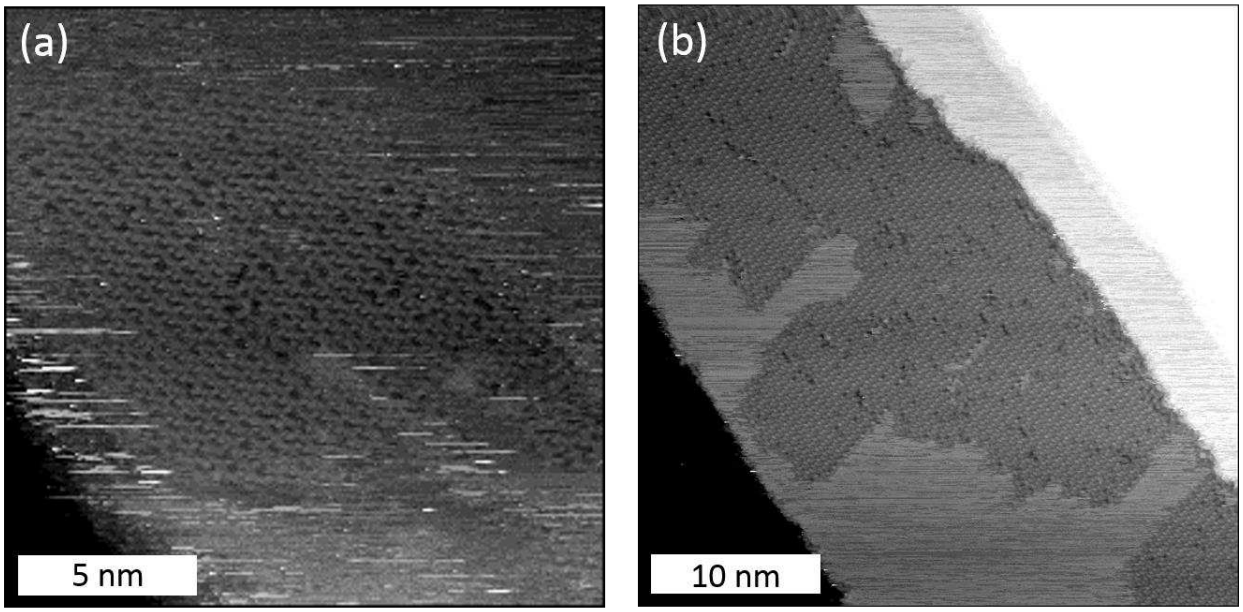

Figure S1. Overview STM images acquired after RT deposition of Br_4F_6BP onto Ag(111), showing (a) more loosely (corresponding to Fig. 2(a) of the main text) and (b) more densely (corresponding to Fig. 2(b) of the main text) packed arrangements of 1D organometallic chains; Interestingly, the average chain lengths as derived from these images are relatively similar, corresponding to (a) (12.7 ± 11) nm and (b) (14.7 ± 13.6) nm (b). (tunneling parameters: (a) 0.09 V, 115 pA; (b) 0.91 V, 91 pA)

Overview STM images after annealing

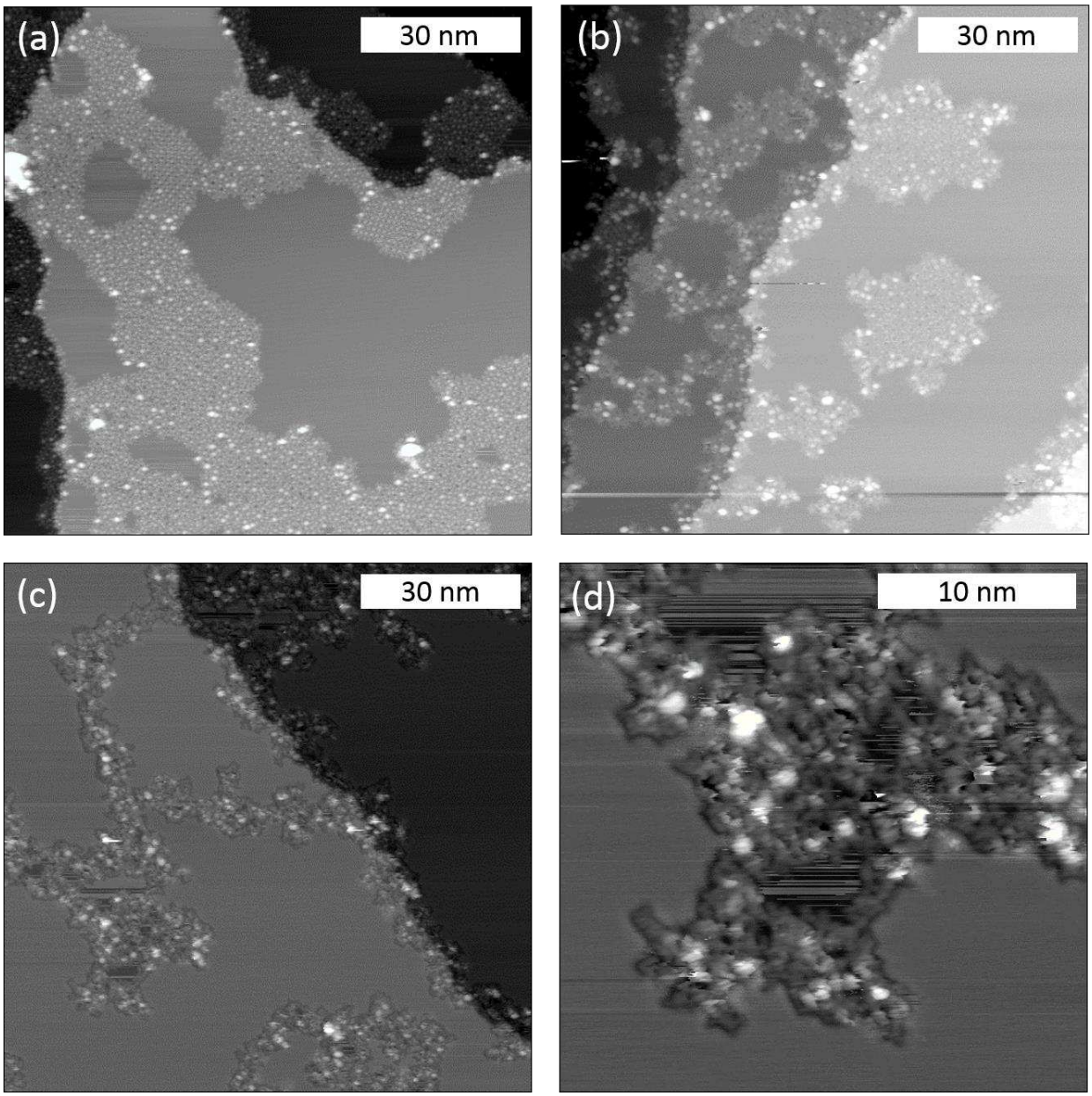

Figure S2. Overview STM images acquired after RT deposition of Br_4F_6BP onto Ag(111) and subsequent annealing to (a) 200 °C, (b) 300 °C, and (c) / (d) 400°C; ordered molecular structures were not resolved anymore after annealing to 400 °C, even though the disordered aggregates appear with relatively uniform height; formation of covalent aggregates is highly plausible, but cannot unambiguously confirmed by these data. (tunneling parameters: all overview images (100 × 100) nm² (a) 0.93 V, 63 pA; (b) 0.88 V, 93 pA; (c) 0.88 V, 90 pA; (d) 0.88 V, 110 pA)

Annealing to 200 °C with reduced heating and cooling rates

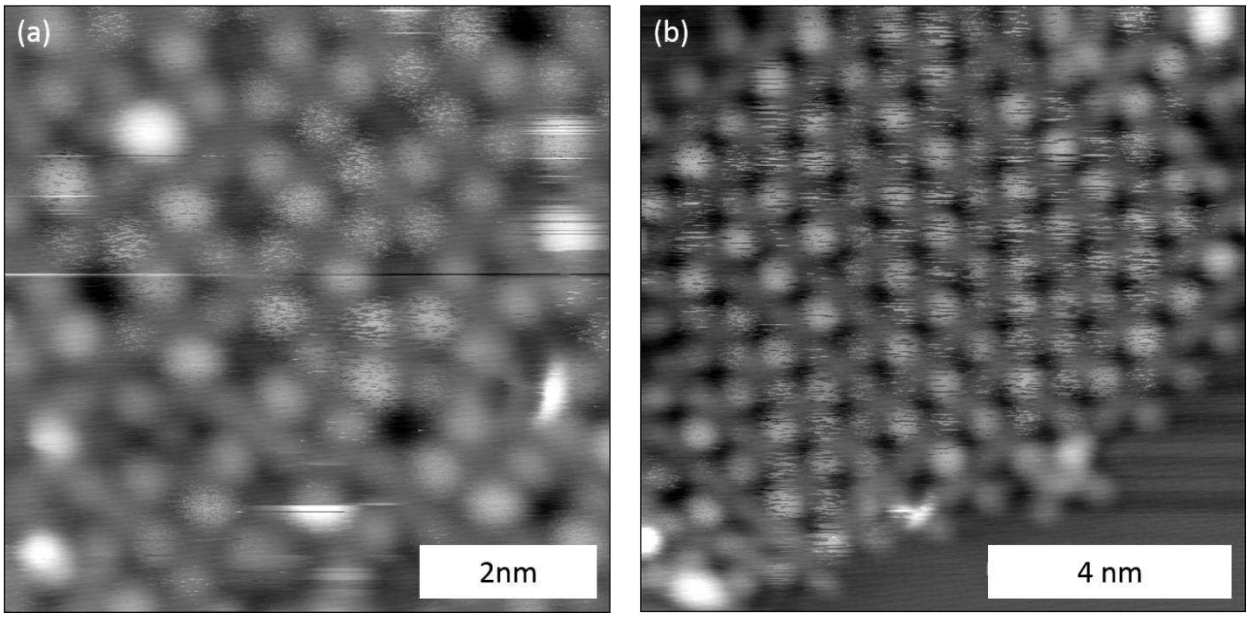

Figure S3. STM images acquired after RT deposition of Br_4F_6BP onto Ag(111) and subsequent annealing to 200 °C with a reduced heating and cooling rate of 1.5 °C min^{-1}. Yet, no differences to heating treatments for the (a) flower and (b) checkerboard structure with the normally applied heating and cooling rate of 5.8 °C min^{-1} could be discerned. (tunneling parameters: (a) 0.71 V, 39 pA; (b) 0.93 V, 45 pA)

Statistical analysis of the 3,5’ site-selectivity

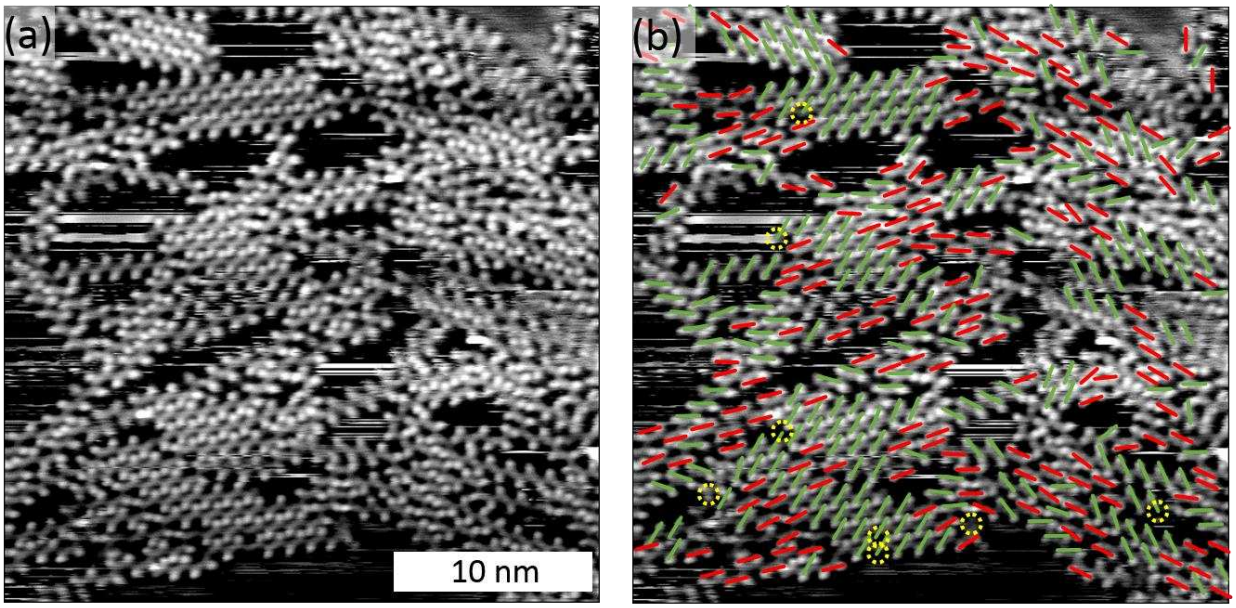

Figure S4. Statistical analysis of a STM image with predmoninatley organometallic chains acquired after room-temperature deposition of Br_4F_6BP onto Ag(111) (corresponding to Fig. 2(a) of the main text); (a) original image; (b) same image with color coding for the site-slectivity: green corresponds to the targeted site-selective 3,5’-didebromaintion (255 counts), whereas red indicates defects with 3,3’-didebromaintion (180 counts); yellow circles show molecules with one remaing bromine substituent. (tunneling parameters: 1.26 V, 22 pA)

Spatial distribution of noisy appearing vs. stably imaged Ag atoms

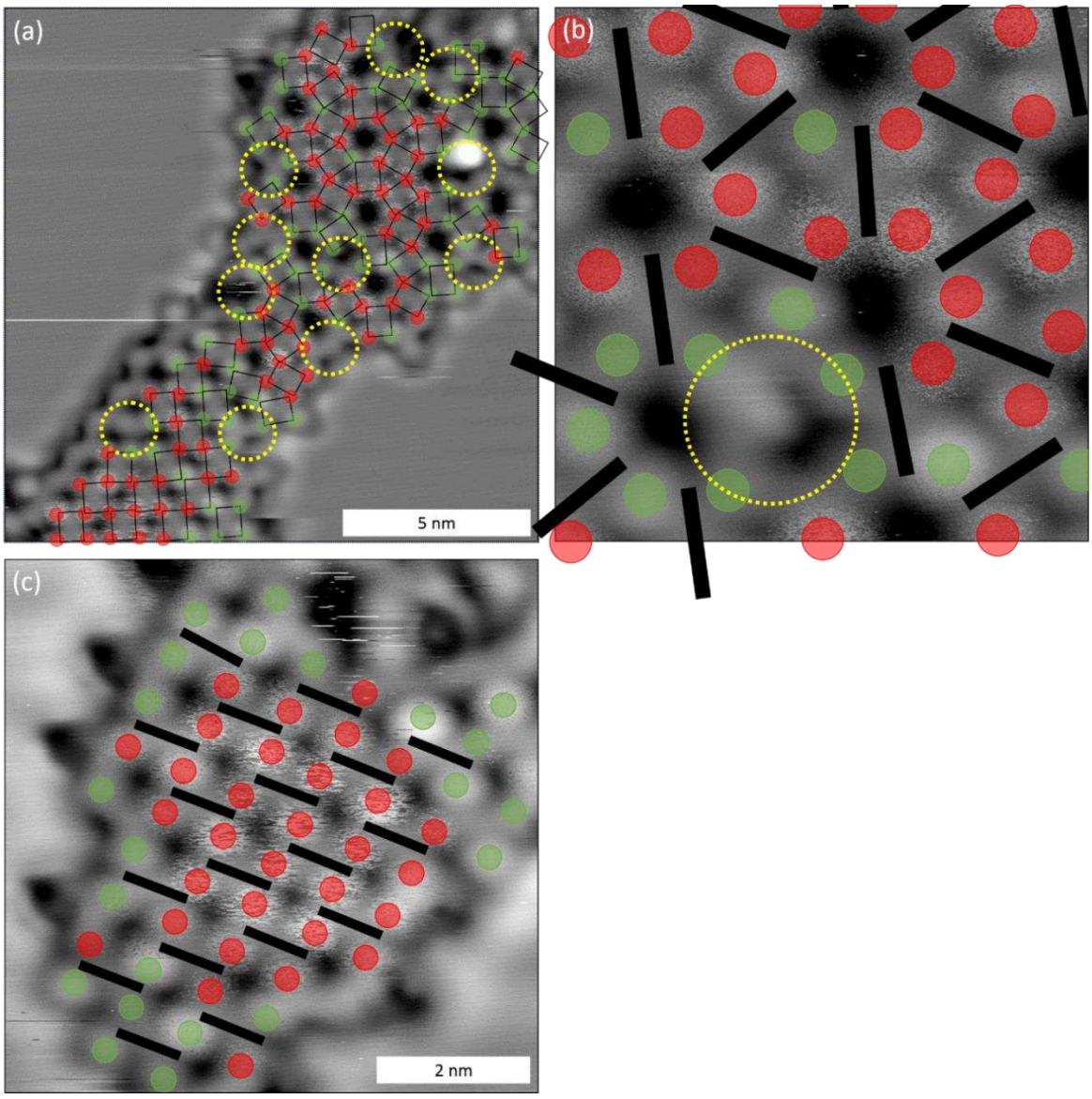

Figure S5. STM images of Br_4F_6BP on Ag(111) acquired after annealing to 200 °C; (a) overview, (b) flower, (c) checkerboard structure; two different types of STM contrast could be distinguished for Ag atoms in the organometallic linkages: **(1)** noisy appearing Ag atoms (red) and **(2)** stable appearing Ag atoms. The color code aids in illustratating the spatial distribution of both contrast types, black bars symbolize biphenyl units. Nosiy Ag atoms are the dominant species within well ordered organometallic domains, whereas stable Ag atoms (green) are mostly located at domain boundaries and around vacancies (marked by yellow circles). (tunneling parameters: (a) 0.58 V, 45 pA; (b) 0.58 V, 45 pA; (c) 0.60 V, 47 pA)

F 1s XP spectra of Br_4F_6BP on Ag(111)

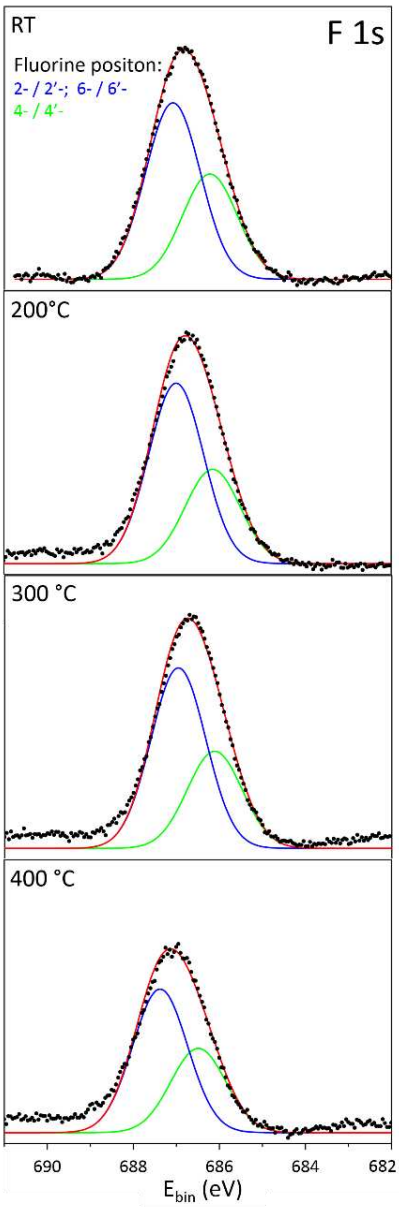

Figure S6. F1s XP spectra acquired after RT deposition of Br_4F_6BP onto Ag(111) and successive annealing to the indicated temperatures up to 400 °C. Raw data are represented by dots; solid lines show fits with Gaussian line-shape and linear background. F 1s spectra were fitted with two components corresponding to the inequivalent fluorine substituents: F at 4- / 4'-position: green; F at 2- / 2'-position and 6- / 6'-position: blue; according to the molecular structure a fixed 1:2 ratio was applied; Annealing at 400 °C already results in a loss of fluorine due to degradation of the molecules by defluorination.

XPS fitting parameters for Br_4F_6BP on Ag(111)

Carbon 1s @RT Fig. 2a						Bromine 3d @RT Fig. 2b				
Peak	Peak type	FWHM	E_B (eV)	rel. Area (%)	Assigned to	Peak type	FWHM	E_B (eV)	rel. Area (%)	Assigned to
1	Gaussian	1.2	283.6	12	C-Ag (½ Br / ½ C-Ag	Gaussian	0.7	68.1	22	Chemisorbed Br (Br $d_{5/2}$)
2	Gaussian	1.2	285.0	20	C-C	Gaussian	0.8	69.1	17	Chemisorbed Br (Br $d_{3/2}$)
3	Gaussian	1.1	285.5	24	C-Br	Gaussian	0.9	70.2	35	Br-C (Br $d_{5/2}$)
4	Gaussian	1.2	286.8	27	C-F (4,4')	Gaussian	1.0	71.3	26	Br-C Br $d_{3/2}$)
5	Gaussian	1.2	286.9	17	C-F (2,6';2',6)					

Carbon 1s @200°C Fig. 2c						Bromine 3d @200°C Fig. 2d				
Peak	Peak type	FWHM	E_B (eV)	rel. Area (%)	Assigned to	Peak type	FWHM	E_B (eV)	rel. Area (%)	Assigned to
1	Gaussian	1.0	283.6	7	C-Ag (½ Br / ½ C-Ag	Gaussian	0.7	68.0	45	Chemisorbed Br (Br $d_{5/2}$)
2	Gaussian	1.0	284.8	28	C-Ag	Gaussian	0.8	69.1	42	Chemisorbed Br (Br $d_{3/2}$)
3	Gaussian	1.0	284.8	3	C-Br	Gaussian	1.2	70.3	9	Br-C (Br $d_{5/2}$)
4	Gaussian	1.0	284.9	18	C-C	Gaussian	0.9	71.4	4	Br-C Br $d_{3/2}$)
5	Gaussian	1.0	286.5	15	C-F (2,6';2',6)					
6	Gaussian	1.0	286.7	30	C-F (4,4')					

Carbon 1s @300°C Fig. 2e						Bromine 3d @300°C Fig. 2f				
Peak	Peak type	FWHM	E_B (eV)	rel. Area (%)	Assigned to	Peak type	FWHM	E_B (eV)	rel. Area (%)	Assigned to
1	Gaussian	1.0	283.6	5	C-Ag (½ Br / ½ C-Ag	Gaussian	0.7	68.1	51	Chemisorbed Br (Br $d_{5/2}$)

2	Gaussian	1.0	284.8	38	C-Ag	Gaussian	0.8	69.1	39	Chemisorbed Br (Br $d_{3/2}$)
3	Gaussian	1.0	284.8	2	C-Br	Gaussian	1.3	70.2	7	Br-C (Br $d_{5/2}$)
4	Gaussian	1.0	284.9	13	C-C	Gaussian	0.9	71.5	2	Br-C Br $d_{3/2}$)
5	Gaussian	1.0	286.5	15	C-F (2,6';2',6)					
6	Gaussian	1.0	286.7	27	C-F (4,4')					

Fluorine 1s RT					
Peak	Peak type	FWHM	E_B (eV)	rel. Area (%)	Fluorine position assigned to
1	Gaussian	1.5	686.2	37	4- / 4'-
2	Gaussian	1.5	687.1	63	2- / 2'-; 6- / 6'-
Fluorine 1s 200°C					
Peak	Peak type	FWHM	E_B (eV)	rel. Area (%)	Fluorine position assigned to
1	Gaussian	1.5	686.1	34	4- / 4'-
2	Gaussian	1.5	687.0	66	2- / 2'-; 6- / 6'-
Fluorine 1s 300°C					
Peak	Peak type	FWHM	E_B (eV)	rel. Area (%)	Fluorine position assigned to
1	Gaussian	1.5	686.1	35	4- / 4'-
2	Gaussian	1.5	687.0	65	2- / 2'-; 6- / 6'-
Fluorine 1s 400°C					
Peak	Peak type	FWHM	E_B (eV)	rel. Area (%)	Fluorine position assigned to
1	Gaussian	1.5	686.5	37	4- / 4'-
2	Gaussian	1.5	687.4	63	2- / 2'-; 6- / 6'-

2. Additional STM data: Br_4BP on Ag(111)

Chain formation *via* site-selective 3,5'-didebromination and influence of surface temperature

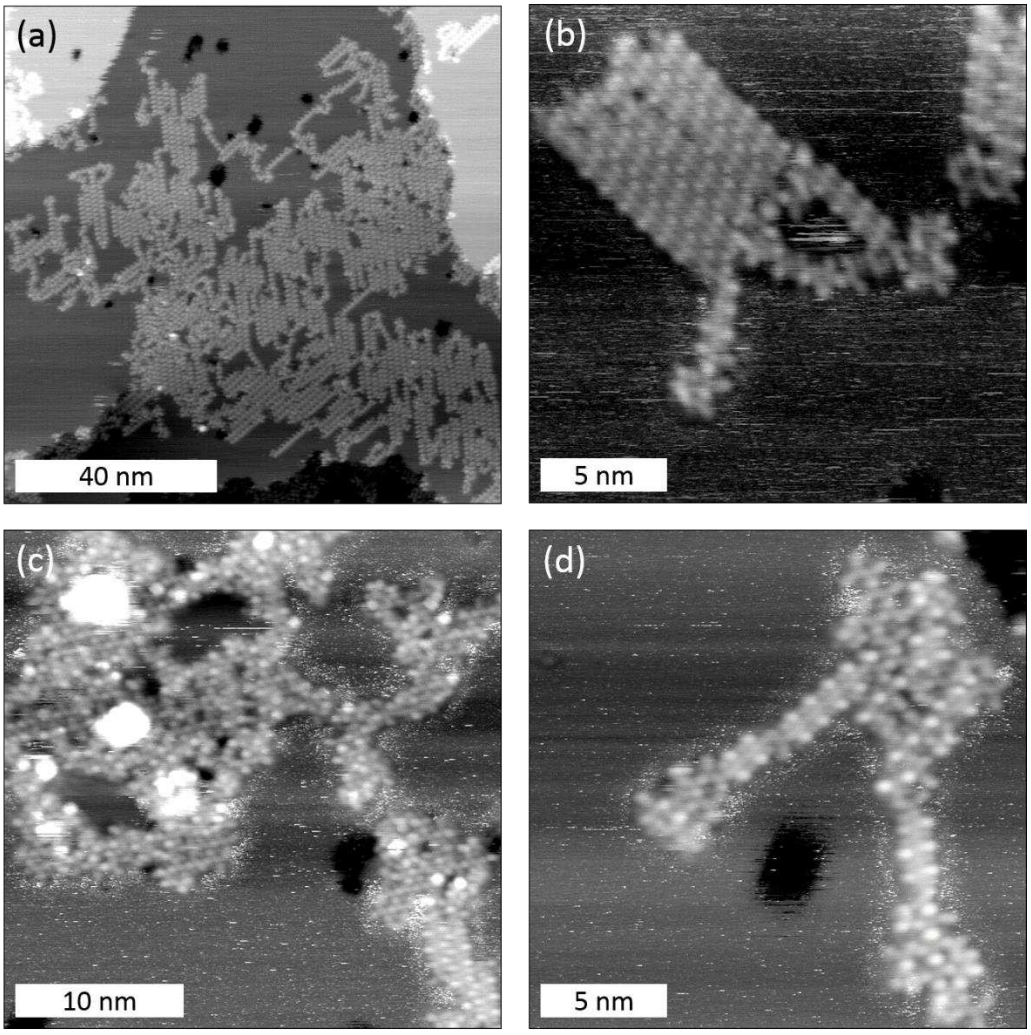

Figure S7. STM images acquired after deposition of non-fluorinated Br_4BP onto Ag(111) with (a) / (b) the surface held at RT and (c) / (d) the surface preheated to 50°C; (a) overview image showing the formation of linear structures, more clearly resolved as organometallic chains in the close-up in (b); the repeat distance of (1.06 ± 0.04) nm perfectly matches the Br_4F_6BP derived organometallic chains; Yet, the chain formation by site-selective 3,5'-didebromination is highly sensitive on the surface temperature as shown in (c) and (d): deposition onto Ag(111) preheated to 50 °C induces a higher density of defects and also leads to the first expression of 2D patterns by progressive debromination; only short segments of organometallic chains are still observed; (tunneling parameters: (a) 0.86 V, 94 pA; (b) 0.48 V, 93 pA; (c) 1.49 V, 95 pA; (d) 1.49 V, 96 pA).

STM images of Br_4BP on Ag(111) after annealing

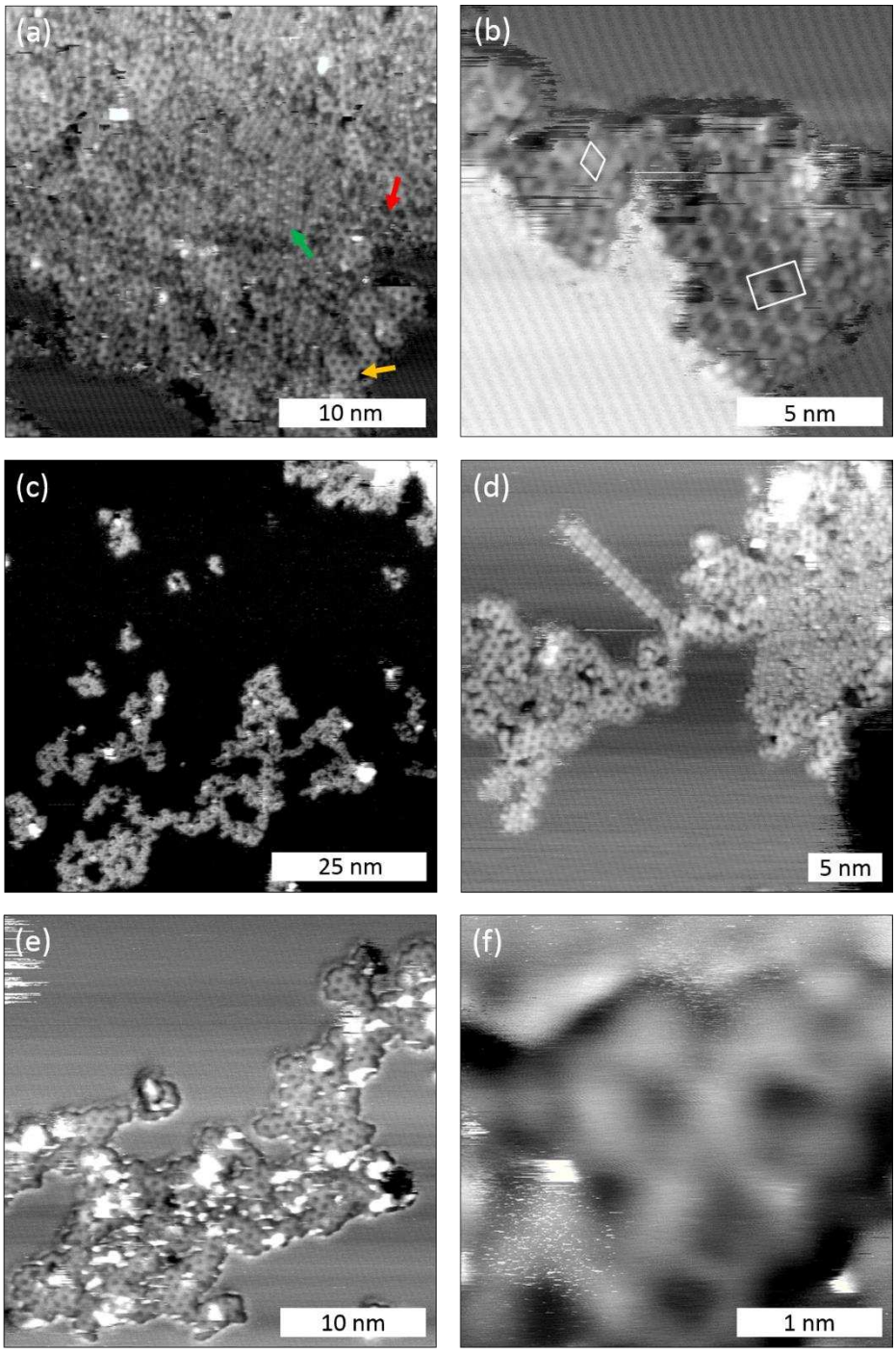

Figure S8. STM images of Br_4BP on Ag(111) acquired after subsequent annealing to (a) / (b) 200 °C; (c) / (d) 300 °C; (e) / (f) 400 °C, with a heating and cooling rate of 3.33 °C min^{-1}. After annealing at 200°C three different structures can be observed by STM: (1) 1D organometallic chains (green arrow), (2) small patches of the centered rectangular

organometallic checkerboard structure (red arrow in (a), white rectangle in (b)) with lattice parameters of a = (1.75 ± 0.10) nm, b = (1.20 ± 0.07) nm that are within the experimental error identical to the Br_4F_6BP derived checkerboard structure; (3) a porous hexagonal structure with a = b = (0.83 ± 0.06) nm (yellow arrow in (a), white diamond in (b)) whose lattice parameters could not be match with any of the Br_4F_6BP derived structures, but corresponds to a covalent checkerboard structure that is identical to the "porous graphene" previously reported by Fasel and coworkers;[1] upon further annealing the 1D chains are progressively replaced by the organometallic checkerboard pattern, yet with relatively small domain sizes and a high amount of more disordered areas; subsequently, the organometallic structures are converted into covalent structures, as deduced from the change of lattice parameters; In contrast to Br_4F_6BP, for Br_4BP large areas of the surface are covered by closed layers of dissociated Br (see striped structures in (b)); the origin of this interesting difference is not clear, but might account for the high disorder and small domain sizes in the organometallic self-assembly of Br_4BP; (tunneling parameters: (a) 0.89 V, 85 pA; (b) 0.89 V, 84 pA; (c) 1.10 V, 94 pA; (d) 1.52 V, 95 pA; (e) 1.27 V, 91 pA; (f) 1.27 V, 91 pA)

3. Additional DFT simulations

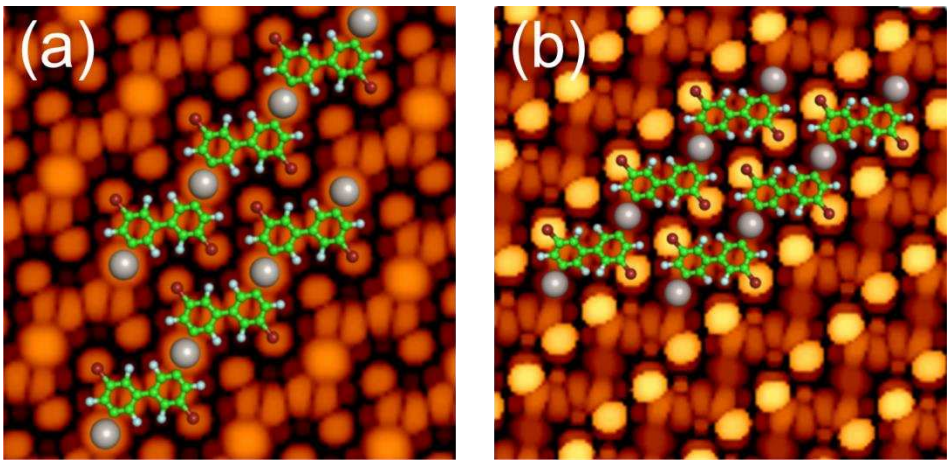

Figure S9. STM image simulations of free-standing organometallic chains, i.e. without Ag(111) substrate. (a) geometry constrained to planar; (b) only Ag atoms constrained to similar height, resulting in a tilting of the phenyl rings in the biphenyl unit with a dihedral angle of ~49°. In the adsorbed state for a symmetric geometry, the phenyl tilt angle with respect to the surface is given by half of the dihedral angle. The underlying DFT-optimized structures are shown as overlays.

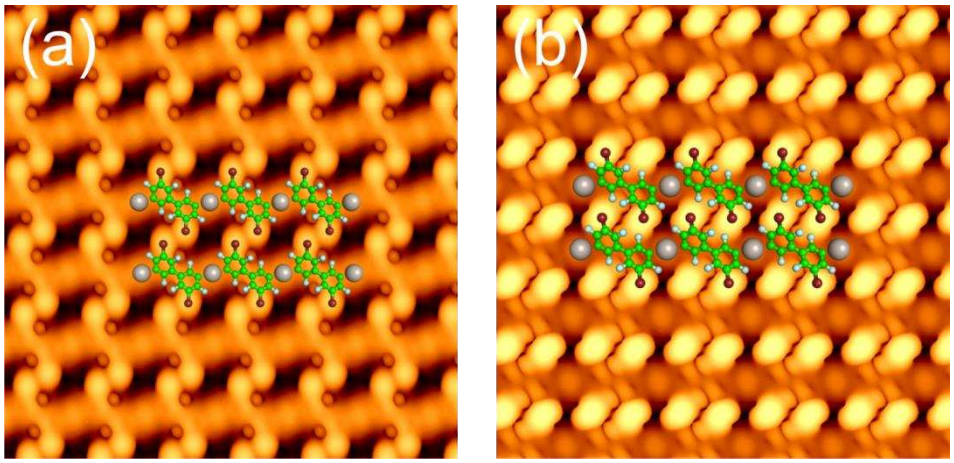

Figure S10. STM image simulations of adsorbed organometallic chains including the Ag(111) substrate; the underlying DFT-optimized structures are shown as overlays: (a) less densely packed structure with a repeat distance along the chain of 1.05 nm and a similar chain separation of 1.05 nm (b) more densely packed structure with a repeat distance along the chain of 1.05 nm and a chain separation of 0.78 nm; in both structures the phenyl rings remain tilted with respect to the surface; the simulated STM images match well with the experiment;

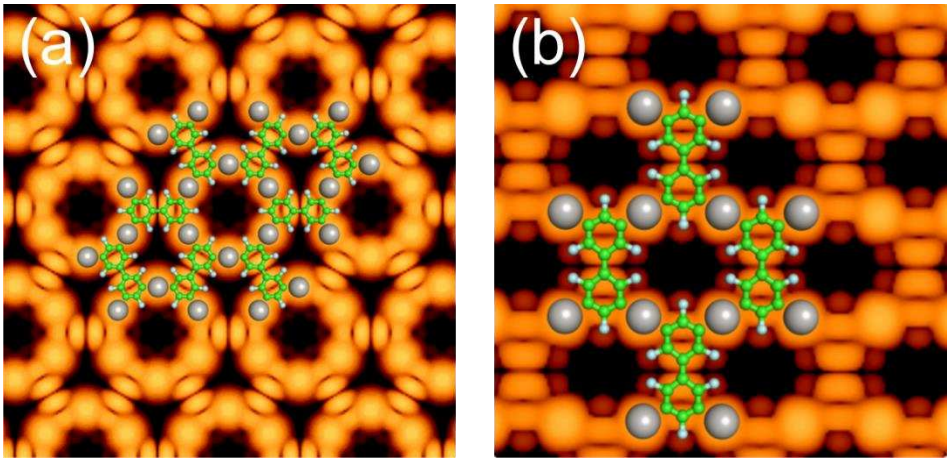

Figure S11. STM image simulations of both organometallic (a) flower and (b) checkerboard structure. The underlying DFT-optimized structures with enforced planar geometry are shown as overlays. In both cases, the Ag atoms in the C-Ag-C linkages appear with a pronounced contrast in accordance with the experiment.

4. Additional STM and XPS data of Br_4F_6BP on Au(111)

STM images of Br_4F_6BP on Au(111)

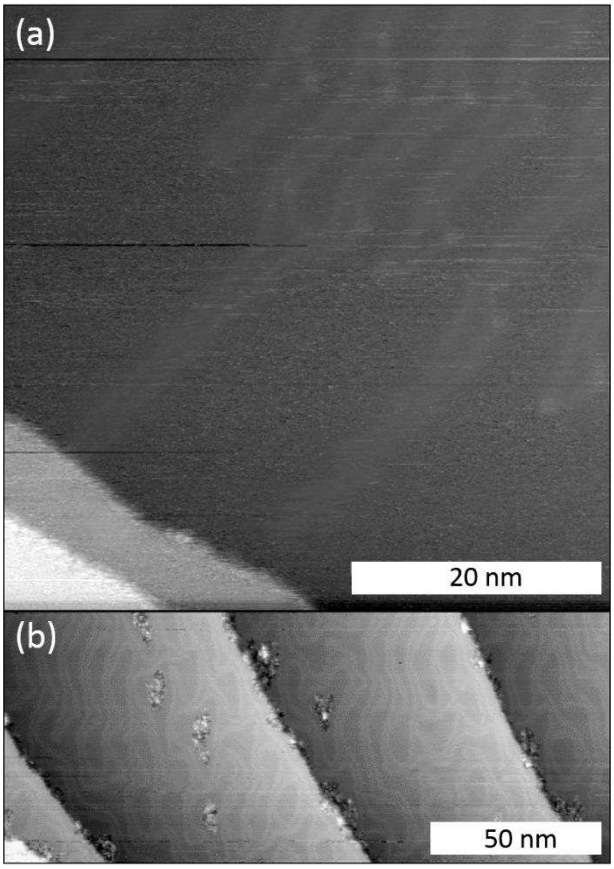

Figure S12. STM data acquired after deposition of Br_4F_6BP on Au(111) at (a) RT and (b) after annealing to 200 °C. At RT, the intact monomers are too mobile to be imaged with STM and the surface appears empty, even though the herringbone reconstruction is locally perturbed. Upon annealing, the majority of molecules was desorbed (cf. XPS in Fig. S13), yet not further resolved aggregates were found scattered across the surface. (tunneling parameters: (a) 1.54 V, 48 pA; (b) 0.98 V, 82 pA).

C 1s and Br 3d XP spectra of Br_4F_6BP on Au(111)

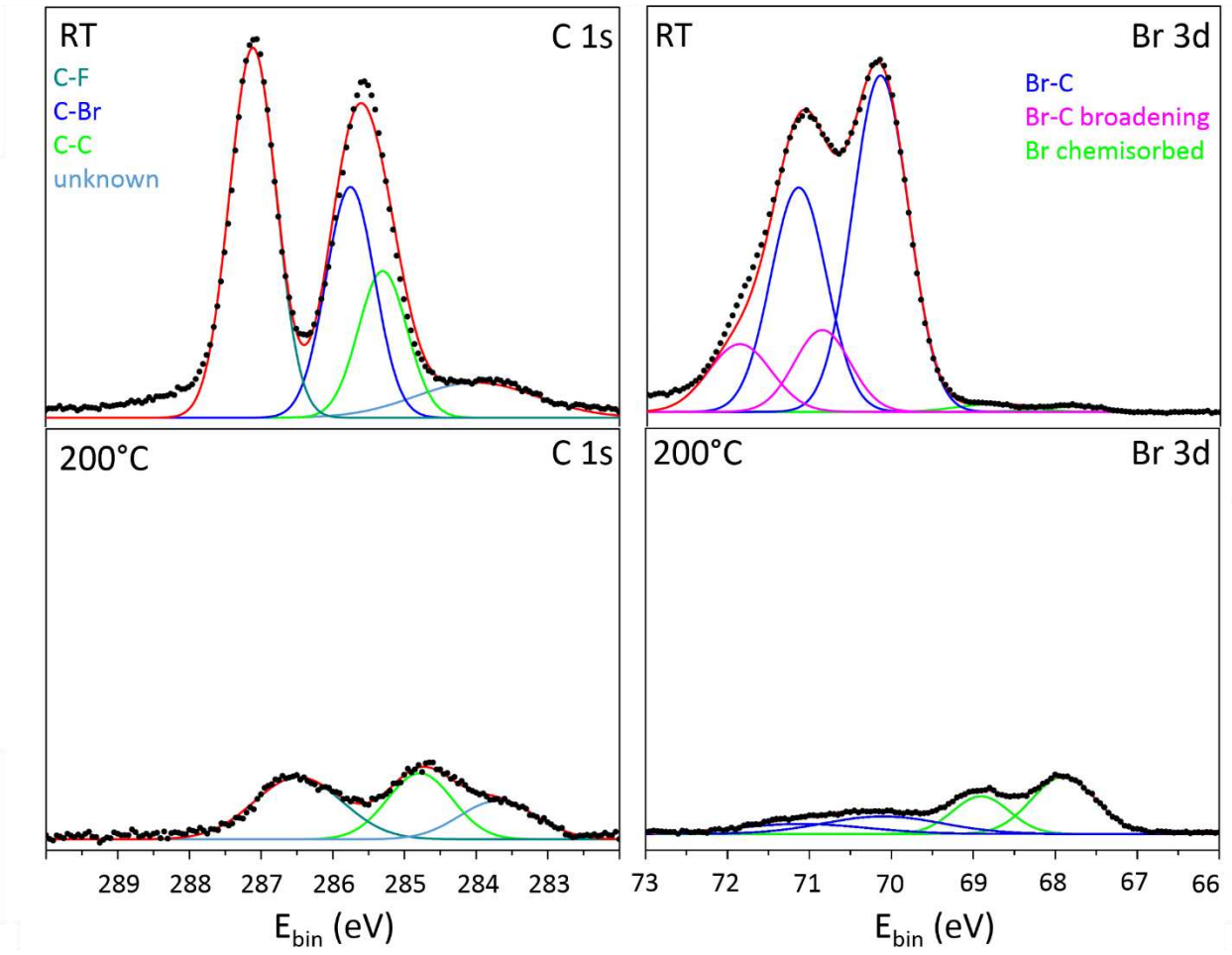

Figure S13. C 1s and Br 3d XP spectra acquired after deposition of Br_4F_6BP onto Au(111) at (a) RT and (b) after annealing to 200 °C. At RT almost no Br substituents were dissociated, hence mostly intact monomers are present on the surface. Obtaining a reasonable fit required an additional Br 3d doublet with a higher binding energy, accounting for 21% of the total intensity. This additional Br species is tentatively assigned to either molecules in special adsorption sites (e.g. step-edges) or second layer coverage, but the exact origin remains unclear at the moment. After annealing, most molecules and Br desorbed, with small remainders of a carbonaceous species and split off Br still present. Raw data are represented by dots; solid lines show fits (fitted with a Gaussian line shape and linear background), where red lines corresponds to the sum of all components.

XPS fitting parameters for Br_4F_6BP on Au(111)

Carbon 1s @RT						Bromine 3d @RT				
Peak	Peak type	FWHM	E_B (eV)	rel. Area (%)	Assigned to	Peak type	FWHM	E_B (eV)	rel. Area (%)	Assigned to
1	Gaussian	2	284	11	-	Gaussian	1	67.8	1	Chemisorbed Br (Br $d_{5/2}$)
2	Gaussian	0.8	285.3	18	C-C	Gaussian	1	68.8	1	Chemisorbed Br (Br $d_{3/2}$)
3	Gaussian	0.8	285.8	28	C-Br	Gaussian	0.8	70.2	46	Br-C (Br $d_{5/2}$)
4	Gaussian	0.8	287.1	43	C-F	Gaussian	0.8	70.9	11	Br-C (Br $d_{5/2}$) broadening
5						Gaussian	0.8	71.2	31	Br-C Br $d_{3/2}$)
6						Gaussian	0.9	71.9	10	Br-C Br $d_{3/2}$) broadening

Carbon 1s @200°C						Bromine 3d @200°C				
Peak	Peak type	FWHM	E_B (eV)	rel. Area (%)	Assigned to	Peak type	FWHM	E_B (eV)	rel. Area (%)	Assigned to
1	Gaussian	1.3	283.7	23	-	Gaussian	0.9	67.8	40	Chemisorbed Br (Br $d_{5/2}$)
2	Gaussian	1.1	284.8	33	C-C	Gaussian	0.8	68.9	29	Chemisorbed Br (Br $d_{3/2}$)
3	Gaussian	1.4	286.5	43	C-F	Gaussian	1.7	70.1	23	Br-C (Br $d_{5/2}$)
4						Gaussian	1.9	71.1	14	Br-C (Br $d_{3/2}$)

5. Synthesis details

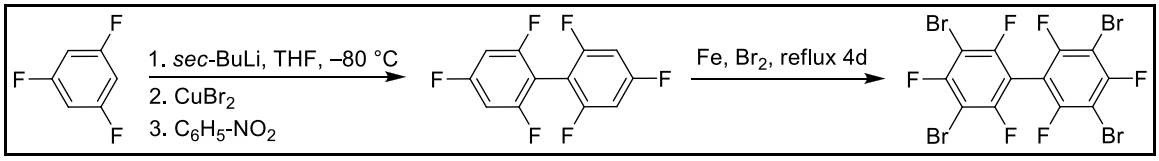

(1) Synthesis of Br_4F_6BP was accomplished after Leroux *et al.*:[2] At –80 °C *sec*-butyllithium (38.6 mmol) in cyclohexane (30.0 mL) was added dropwise to a solution of 1,3,5-trifluorobenzene (5.10 g, 3.90 mL, 38.6 mmol) in tetrahydrofuran (90.0 mL). After completion of the addition, stirring was continued for 3 h under nitrogen atmosphere. Still at –80 °C copper-(II)-bromide (8.60 g, 38.6 mmol) was added in one portion under vigorous stirring and 45 minutes later nitrobenzene (4.75 g, 4.00 mL, 38.6 mmol) was added dropwise. The reaction mixture was brought to room temperature overnight and filtered through a column of basic alumina (100 g). The filter cake was eluted with n-hexane. After evaporation of all volatiles the residue was purified by column chromatography on flash-silica with *n*-hexane. Further purification by vacuum-sublimation (80 °C .. 90 °C at 0.01 mbar) afforded a colorless powder. Yield: 7.10 g (70%). ^{1}H NMR (400 MHz, CDCl3): δ 6.80 (m, 4H).

(2) Synthesis of Br_4F_6BP was prepared after Sakamoto *et al.*:[3] At 0 °C bromine (7.00 mL, 21.8 g, 136 mmol) was added to a mixture of 2,2',4,4',6,6'-hexafluorobiphenyl (2.00 g, 7.63 mmol) and iron powder (1.50 g, 26.9 mmol). After removal of the ice bath the reaction mixture was refluxed for 4 days. At room temperature the reaction mixture was poured into aqueous sodium thiosulfate solution and was extracted with dichloromethane. The organic phase was washed with brine and dried over sodium sulphate. After evaporation of the volatiles the residual solid was recrystallized from ethanol. Subsequent vacuum sublimation (90 °C .. 110 °C at 0.01 mbar) afforded a colorless powder. Yield: 2.42 g (55%). Mp: 162 °C. IR (KBr, cm^{-1}): 1599 (s), 1427 (s), 1056 (s), 765 (s), 706 (s), 639 (w), 589 (s), 568 (s). ^{19}F NMR (564 MHz, $CDCl_3$): δ 70.4 (m, 4F), 60.3 (m, 2F). ^{13}C NMR (100 MHz, $CDCl_3$): δ 158.0 (d, 1J = 250 Hz), 156.4 (d, 1J = 250 Hz), 102.8, 95.0. Anal. Calcd for $C_{12}Br_4F_6$: C, 24.95. Found: C, 25.20

^{13}C-NMR: (100 MHz, $CDCl_3$): Br_4F_6BP

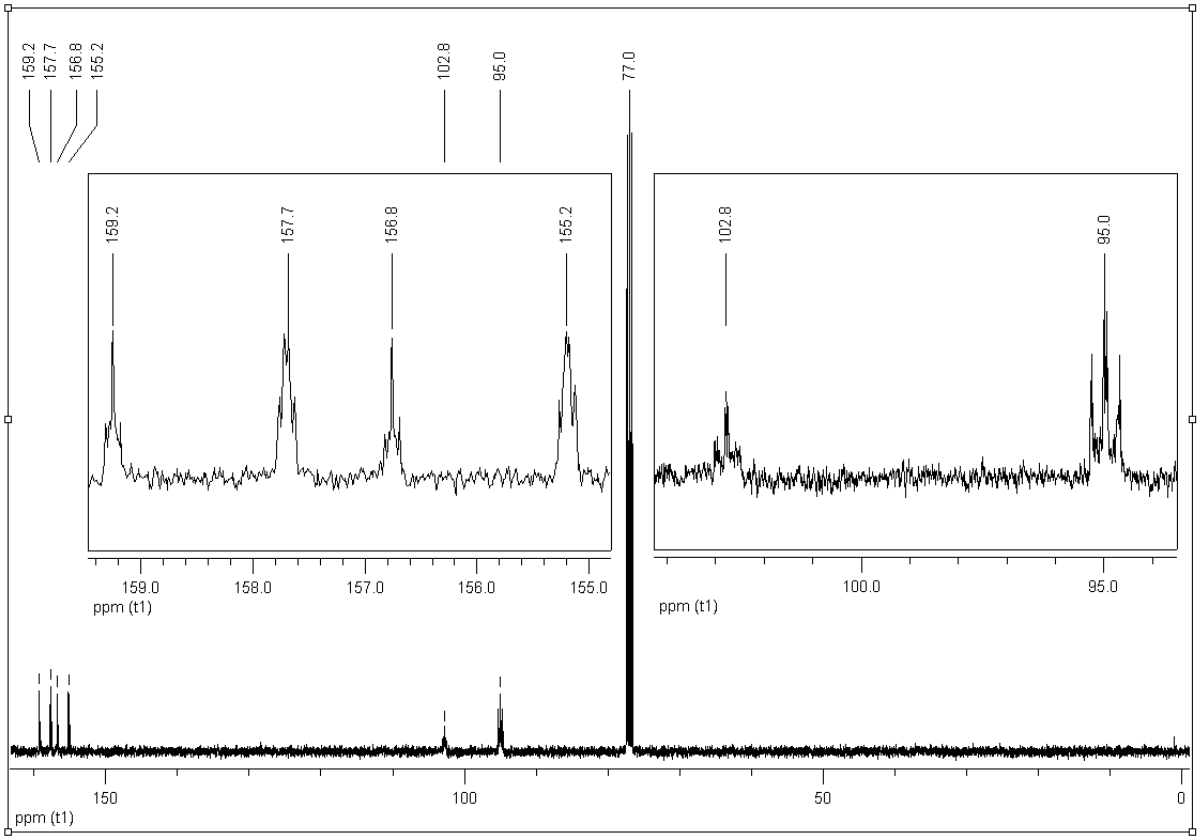

^{19}F-NMR (564 MHz, $CDCl_3$): Br_4F_6BP

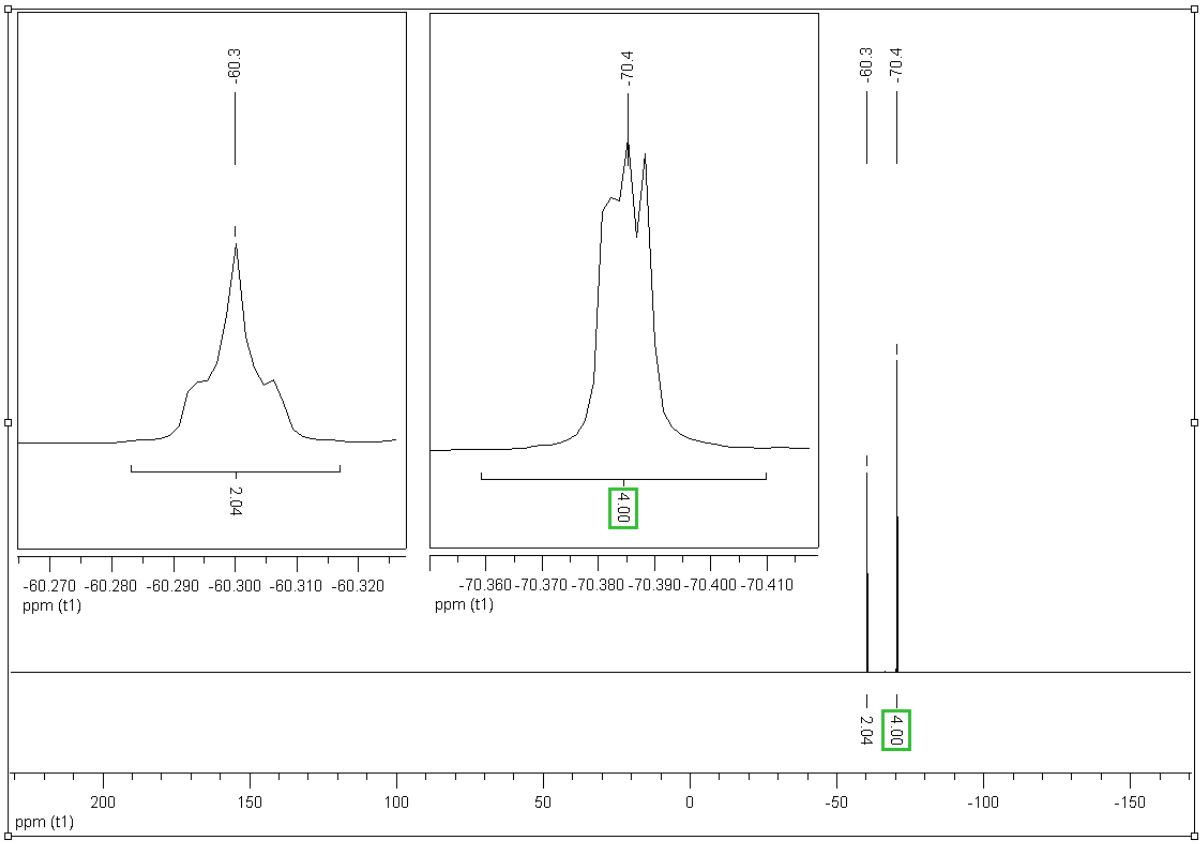

References

1. M. Bieri, M. Treier, J. Cai, K. Aït-Mansour, P. Ruffieux, O. Gröning, P. Gröning, M. Kastler, R. Rieger, X. Feng, K. Müllen and R. Fasel, *Chem. Commun.*, 2009, **0**, 6919-6921.
2. F. Leroux, R. Simon and N. Nicod, *Lett. Org. Chem.*, 2006, **3**, 948-954.
3. Y. Sakamoto, T. Suzuki, A. Miura, H. Fujikawa, S. Tokito and Y. Taga, *J. Am. Chem. Soc.*, 2000, **122**, 1832-1833.